Article

Online battery-protective vehicle to grid behavior management

Shuangqi Li[1, 2], Pengfei Zhao[3], Chenghong Gu[2], Da Huo[4], Xianwu Zeng[2], Xiaoze Pei[2], Shuang Cheng[2], Jianwei Li[2]

[1] National Engineering Laboratory for Electric Vehicles, School of Mechanical Engineering, Beijing Institute of Technology, Beijing 100081, China

[2] Department of Electronic and Electrical Engineering, University of Bath, Bath, UK

[3] The State Key Laboratory for Management and Control of Complex Systems, Institute of Automation, Chinese Academy of Sciences, Beijing 100190, China

[4] School of Water Energy and Environment, Cranfield University, Cranfield, UK

Abstract: With the popularization of electric vehicles, vehicle-to-grid (V2G) has become an indispensable technology to improve grid economy and reliability. However, battery aging should be mitigated while providing V2G services so as to protect customer benefits and mobilize their positivity. Conventional battery anti-aging V2G scheduling methods mainly offline operates and can hardly be deployed online in hardware equipment. This paper proposes a novel online battery anti-aging V2G scheduling method based on a novel two-stage parameter calibration framework. In the first stage, the V2G scheduling is modeled as an optimization problem, where the objective is to reduce grid peak-valley difference and mitigate battery aging. The online deployment of the developed optimization-based V2G scheduling is realized by a rule-based V2G coordinator in the second stage, and a novel parameter calibration method is developed to adjust controller hyper-parameters. With the parameter calibration process, the global optimality and real-time performance of V2G strategies can be simultaneously realized. The effectiveness of the proposed methodologies is verified on a practical UK distribution network. Simulation results indicate that it can effectively mitigate battery aging in providing V2G services while guaranteeing algorithm real-time performance.

Keywords: Battery degradation; battery protective strategy; electric vehicle; energy management; energy storage system; transportation electrification; vehicle to grid.

I. Introduction

In recent years, there has been an increasing demand for transportation electrification in response to the need for a more economical and environmentally friendly urban energy system [1]. Electric vehicles, as one of the most important components of the modern transport system, have been greatly promoted to reduce greenhouse gas emissions and fossil fuel consumption [2, 3]. The penetration of electric vehicles, specifically, the energy storage capacity in the battery of grid-connected electric vehicles (GEVs) provides a new solution for improving the economy, efficiency, and stability of the power grid [4]. According to [5], only 4% lifetime of electric vehicles is used for transportation, while most are spent in parking lots and garages. Known as vehicle to grid (V2G) services, the energy storage in GEVs can be used to provide power balancing [6, 7], frequency regulation [8, 9], and voltage control services [10] to the power grid. Numerous studies in existing literature have explored the optimal operation of the power grid with GEVs and renewable energy penetrations [11-13].

Compared to the frequency and voltage regulation, the peak-shaving service is of great significance to the modern urban energy system with large-scale renewable energy penetration [14, 15]. The GEVs can be used to reduce grid peak-valley difference and improve grid energy utilization efficiency by deferring their charging demand in time or even in space and acting as dynamic storage devices [16, 17]. However, different from frequency and voltage regulation service, the battery of GEVs may undergo many deep cycles that harm their longevity when providing peak-shaving service to the grid [18]. In recent years, many studies have been conducted to mitigate the battery aging in V2G scheduling [19, 20].

The rule-based algorithm is one of the most commonly used V2G scheduling methods because of its remarkable real-time performance and hardware applicability [21, 22]. In the rule-based V2G scheduling method, the target of battery aging mitigation is usually realized by limiting battery depth of discharge (DOD) and discharging rate (C-rate) in the controller [23]. An event-based dynamic V2G scheduling method is developed in [24] for aggregators and charging pile control in large-scale V2G applications in GEV car parks. V2G behaviors are controlled by a series of underlying rules that reflect the charging requirement of GEVs, and the aging is mitigated by limiting the C-rate and DOD of vehicle battery during participating in providing services. In [25], the fuzzy logic algorithm is further used to schedule the charging behavior of GEVs, and the DOD is subjected to fuzzy rules to protect the battery from over-discharging and charging. The C-rate and DOD constraints are adopted in rule-based V2G scheduling methods to mitigate battery aging. However, because the vehicle battery is an integrated electrochemical system with complex aging mechanisms, the shallow external characteristics can hardly comprehensively and accurately capture its aging factors [26]. Therefore, battery aging is not able to be effectively suppressed in rule-based methods.

The optimization-based scheduling method is employed in some latest researches to further reduce the battery aging cost in V2G scheduling, in which the battery anti-aging is designed as optimization objectives on large time scales [27-30]. A day-ahead V2G scheduling model is developed in [31] to coordinate the charging behavior of GEVs in a residential area. The aging cost of the battery is modeled as a function of surface temperature, average current rate, battery number of cycles (NOC), and DoD. The stochastic optimization algorithm is employed to derive the optimal V2G strategies, and simulation results indicated that the developed scheduling method could mitigate the battery degradation phenomenon when participating in V2G services. In a further study [32], a practical wear cost model is established to evaluate the battery anti-aging performance of V2G strategies, and the minimization of battery aging cost is designed as an optimization objective in a mixed-integer linear programming model. The effectiveness of the developed method is verified in several case studies, and simulation results indicated that the integration of the practical wear cost model and linear programming model could effectively mitigate battery aging in V2G scheduling.

Due to the use of large-scale optimization algorithms and comprehensive aging models, battery degradation can be effectively suppressed by using optimization-based scheduling methods [33]. However, for the same reason, the real-time performance of the optimization-based model is usually not satisfactory and thus can hardly be used in hardware in the real world [34]. Rule-extraction is one of the most commonly used methods to deploy the strategies from the optimization model [35, 36]. In [37], the energy management strategy of electric vehicles derived by a dynamic programming algorithm is deployed in vehicle controllers by a rule-extraction model. Experimental results indicated that the recalibrated rule-based model could manage the online operation of vehicle power systems while achieving a similar comprehensive performance compared to the dynamic programming model. Combined with the rule extraction method, the optimal V2G strategies derived in the optimization-based model can be deployed in charging devices in the real world. However, to the authors' best knowledge, there is no published work on applying the rule extraction method to optimal V2G scheduling.

To resolve the aforementioned problems, this paper develops an optimal V2G scheduling method that can mitigate battery aging while reserving the real-time performance of the developed algorithm. Firstly, based on daily operation information of the power grid, including load profiles and GEVs charging requirements, the optimal charging strategies are scheduled by an optimization-based V2G scheduling model. In the optimization, the peak-shaving requirement of the power grid and battery anti-aging requirement of V2G participants is considered. Then, a novel online V2G coordinator is established by extracting rules from the derived optimal strategies in the optimization-based scheduling model. The calibrated rule-based controller is used to manage the charging and discharging behaviors of GEVs. The built rule-based controller can provide similar peak-shaving and battery anti-aging V2G strategies compared to the optimization-based model but avoid using complex optimization processes. The key contributions of this paper are summarized as follows:

1) This paper is the first attempt to explore the online deployment of battery anti-aging V2G strategies. The grid peak-shaving requirement, mitigating of battery aging, and real-time performance of scheduling algorithm are comprehensively handled.
2) A novel two-stage parameter calibration framework is designed for V2G scheduling, which overcomes the shortages of optimization-based and rule-based scheduling methods by using the parameter calibration process to adjust controller hyper-parameters. The global optimal strategies and real-time applicability can be

simultaneously achieved.

3) It comprehensively considers the grid peak-shaving requirement and battery anti-aging requirements in a novel optimization-based V2G behavior management model. With the developed optimization model, the optimal V2G strategies can be achieved.
4) A novel parameter calibration method is developed to adjust hyper-parameters in the rule-based V2G coordinator that is used to schedule the charging behavior of GEVs online. After the parameter calibration process, the established rule-based coordinator can reproduce the optimal V2G strategies derived in the optimization-based scheduling model in real-time.

The rest of the paper is organized as follows: The developed two-stage parameter calibration framework is discussed in Section II. Section III presents the developed optimization-based V2G management model. The developed online rule-based V2G coordinator and the parameter calibration method are in Section IV. The simulation platform and the performance of the proposed V2G scheduling method are evaluated in Sections V, followed by concluding remarks in Section VI.

II. Two-stage parameter calibration framework for V2G scheduling

This section develops a novel two-stage optimization and parameter calibration framework (OPCF) to derive the global optimal V2G strategies and guarantee real-time performance simultaneously.

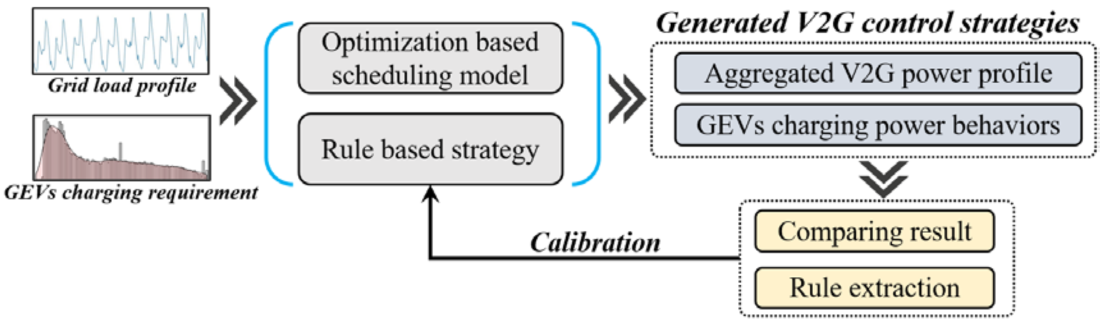

Fig. 1. The two-stage optimization and parameter calibration framework for V2G scheduling.

All GEVs should be synergistically scheduled to improve the quality of peak-shaving services provided by V2G. While to mitigate battery aging in providingV2G service, GEVs charging and discharging should be optimized for a long period. Large-scale optimization should be used to obtain the globally optimal solutions in V2G scheduling. Therefore, as shown in Fig. 1, in the first stage, an offline scheduling model is built, where the optimal V2G behavior management is modeled as a large-scale optimization problem. The reduction of the peak-valley difference and mitigation of battery aging are designed as optimization objectives, while the charging requirements of GEVs are set as constraints. The grid load profiles and vehicle charging requirements are used as the inputs to calculate the V2G power states of all GEVs. The generated V2G strategies, including the aggregated V2G power profile and GEVs charging behaviors, are further saved in a rule base and will then be used as a benchmark to guide the establishment of the online V2G power coordinator. With the developed optimization-based V2G behavior management model, all GEVs can be synergistically scheduled to provide peak-shaving services to the grid, and battery aging can be mitigated in the whole scheduling period.

The globally optimal V2G strategy can be derived from the established optimization-based scheduling model. However, the use of the large-scale optimization algorithm makes it hardly be used in charging devices in the real world. To enable online scheduling, a fuzzy V2G power controller is established in the second stage, as shown in Fig. 1. The generated V2G control strategies in the rule-based controller are compared with the optimization-based scheduling model. The difference between the two models is used as a feedback signal to optimize the parameters of the rule-based model further.

With the above-developed OPCF method, the optimal V2G strategy derived by the optimization-based method can be transcribed to the fuzzy controller. Therefore, both optimal scheduling performance and real-time control can be realized at the same time. In the rest of the paper, the mathematical principle of the developed optimization-based V2G scheduling method, the fuzzy V2G power coordinator, and the parameters calibration method will be detailed.

III. Optimization-based V2G behavior management model

This section presents an offline optimization-based behavior management model to derive the optimal V2G strategies that can schedule GEVs to provide grid peak-shaving service and mitigate the battery aging simultaneously.

As a type of distributed energy storage system, GEVs can stabilize grid operation by consuming energy from the grid or providing it back. Demand from the grid side is mainly about realizing load shifting, and demand from the user side is to complete EV charging within the set deadline while at the same time minimizing battery degradation caused by V2G service. The V2G scheduling essentially is an optimization problem that coordinates the charge/discharge power for each GEVs. The optimal solutions can be obtained by using the optimization algorithm with several objective functions and constraints representing the need of both the grid and user sides. The optimization variable in the developed optimization-based V2G behavior management model is designed as the charging power of GEVs:

$$\mathbf{P}_i^o = \left[P_i^o(1) \quad \cdots \quad P_i^o(t) \quad \cdots \quad P_i^o(n) \right] \tag{1}$$

$$\mathbf{P}^o = \begin{bmatrix} \mathbf{P}_1^o \\ \vdots \\ \mathbf{P}_m^o \end{bmatrix} \tag{2}$$

Where: $\mathbf{P}^o$ is the optimization variable, which consists of V2G power sequences of m GEVs $\mathbf{P}_i^o$; $P_i^o(t)$ is the charging power of GEV_i at t. The first optimization objective is to reduce the grid peak-valley difference:

$$OBJ_{ps} = \sum_{t=1}^{n}\left(P_{load}(t) + \sum_{i=1}^{m} P_i^o(t) - P_{\text{ref}}(t)\right)^2 \tag{3}$$

Where: $P_{load}(t)$ is grid load state at t; P_{ref} is a reference load line that reflects the preferred point-of-loading value. P_{ref} is formulated by grid operators to guide the operation of the power distribution system [38]. In this study, the value of P_{ref} is assumed to be the median load level within the simulation period. In equation (3), the minimization of grid load fluctuation variance is designed as the objective. With this optimization objective function, the V2G strategy $\mathbf{P}^o$ can guide GEVs charging and discharging behaviors to provide peak-shaving service to the grid.

The second optimization objective is to mitigate battery aging in providing V2G services. The battery SoC trajectory of GEVs in V2G scheduling can be calculated by the following equation:

$$SOC_i(t) = SOC_i(t-1) - \frac{P_i^o(t) \bullet T}{Q_i} \times 100\% \tag{4}$$

Where: $SOC_i(t)$ and $SOC_i(t-1)$ are the battery energy state of GEV_i at t and t-1 respectively; Q_i is the battery capacity; T is the duration of a scheduling period. The rain-flow cycle-counting (RCC) algorithm is usually used for analyzing the fatigue data and was firstly used in metal fatigue estimation [39, 40]. In this research, this method is used to extract the irregular charging and discharging cycles from the GEVs battery SoC trajectory in V2G scheduling. Basically, the cycle counting can be achieved by the following three steps:

(1). Firstly, the adjacent points are extracted by distinguishing the local maxima and minima information in the battery SoC trajectory. As shown in Fig. 2, S_1 to S_7 are the extracted adjacent points in a daily V2G power profile. The extracted adjacent points are further used to label the battery DOD and NOC.

(2). Secondly, the battery number of full-cycles (NFC) and the number of half-cycles (NHC) are labeled by analyzing the amplitude and phase of the extracted adjacent points. It is worth noting that all half discharging and charging sub-cycles are added up together to form complete full-cycles in the RCC algorithm to enforce the feasibility of the battery anti-aging.

(3). At last, the battery NOC and the corresponding DOD data (DOD_1 to DOD_4) are extracted for further analysis.

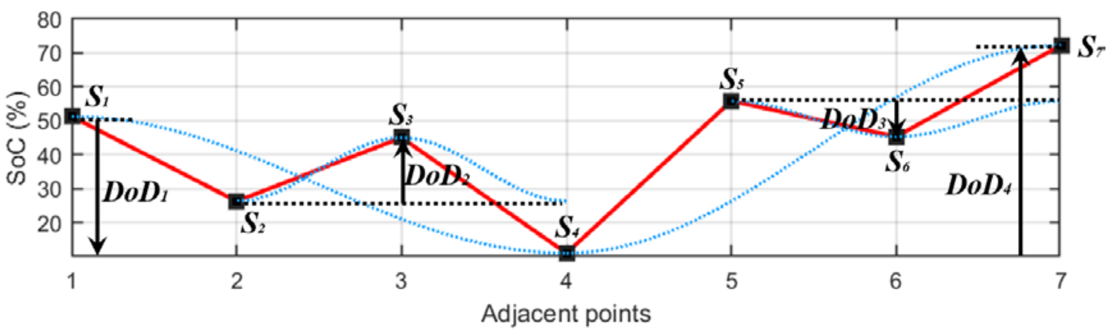

Fig. 2. The extracted battery NOC and DOD in rain-flow cycle counting algorithm.

Based on the extracted battery NOC and DOD information from V2G power time-series, the second V2G optimization objective is designed to reduce battery life loss when participating in V2G services:

$$OBJ_{ag} = \sum_{i=1}^{m} f_{ctf}(NOC_i, DOD_i) \tag{5}$$

Where: NOC_i and DOD_i are the battery NOC and DOD of GEV_i. f_{ctf} is used to calculate percentage battery life loss based on the extracted NOC and DOD of each cycle, and the corresponding cycle-to-failure profile is given in [41]. Based on the above analysis, the following optimization model is established for deriving the optimal V2G strategies:

$$\min_{\mathbf{P}_1^o \ \cdots \ \mathbf{P}_m^o} \ F = \left\{OBJ_{ps}, OBJ_{ag}\right\} \tag{6}$$

By minimizing OBJ_{ps} and OBJ_{ag}, the generated V2G strategies can guide GEVs to provide peak-shaving services to the power grid while mitigating battery aging. The constraints adopted in the defined optimization-based V2G scheduling model are given in Eq. (7) ~ (9):

$$-P_{i,\mathrm{discharg}}^{\max} \le P_i(t) \le P_{i,\,\mathrm{ch\,arg}}^{\max} \tag{7}$$

$$\mathrm{SoC}_{\min} \le \mathrm{SoC}_{i,t} \le \mathrm{SoC}_{\max} \tag{8}$$

$$SoC_i^{\mathrm{end}} \ge SoC_i^{\mathrm{set}} \tag{9}$$

Firstly, the scheduled V2G power should not exceed the maximum discharging power $P_{i,\mathrm{discharg}}^{\max}$ and charging power $P_{i,\,\mathrm{ch\,arg}}^{\max}$ of GEV_i. Then, the lower limit and upper limit of battery energy state are also adopted to protect the battery from over-discharging and overcharging, $\mathrm{SoC}_{\min}$ and $\mathrm{SoC}_{\max}$ of all GEVs are preset as 10% and 95%, respectively. SoC_i^{set} reflects the charging requirement of V2G participants, and the final battery energy state SoC_i^{end} should be higher than the preset value.

Fig. 3 summarizes the inputs, constraints, and objectives employed in the established V2G scheduling model. In summary, the optimal strategy is derived by solving the optimization model with GEV status information as an optimization variable, grid load demand status P_{load} and P_{ref} as optimization inputs, user and GEV charging requirements in Eq. (7) ~ (9) as constraints, and cost function in Eq. (6) as objective. In this study, the cooperative differential evolution algorithm [42], which has been widely used in smart grid energy resource management, V2G scheduling, and smart home energy management, is used to solve the defined optimization model.

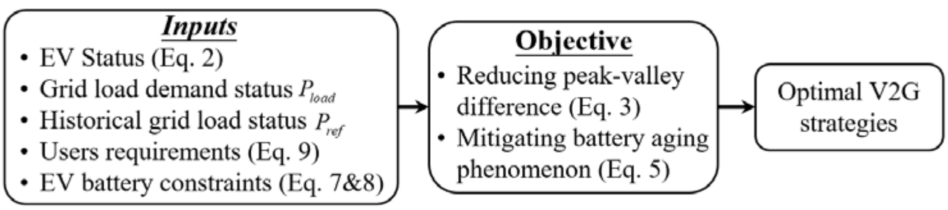

Fig. 3. The established V2G behavior optimization mathematical model.

IV. Online rule-based V2G coordinator

With the developed optimization-based V2G behavior management model, the global optimal strategy can be derived. In this section, a rule-based online V2G power coordinator and a parameter calibration method are developed to enable the deployment of the derived strategy.

A. Online V2G power coordinator

An online fuzzy V2G power coordinator (FVPC) is developed in this section to schedule the behavior of GEVs to provide peak-shaving service to the grid. The two input variables and one output variable are adopted in the designed FVPC:

1) The grid power balance state G, which is used to reflect the peak-shaving and valley-filling requirements and can be calculated by the following equation:

$$G = P_{load} - P_{\text{ref}} \tag{10}$$

2) The vehicle battery state SoC, which is used to reflect the charging requirement of GEVs.
3) The V2G power state P, which is used to control the real-time V2G power of GEVs.

The range of G is normalized to [-1,1] according to the characteristic of power systems. The negative value indicates that the grid demand is low, and the positive value indicates that the appearance of grid demand peaks. The range P is also normalized to [-1,1] according to the rated charging and discharging power of GEVs. The negative value indicates the maximum charging power, while the positive value indicates the maximum discharging power.

The performance of the fuzzy controller is affected by the quality of the membership function. Therefore, the membership functions (MFs) of all fuzzy variables are variable size designed. To simplify the optimization process, all MFs are symmetrically designed in this study. The gauss member function is one of the most commonly used MFs in the fuzzy logic controller for its wide applicability and simple form. Only two parameters are adopted in the gauss member function to describe the characteristics: the standard deviation σ, which is used to describe the position of MFs; and the mean c, which is used to describe the width of MFs. The gauss member function can be depicted by the following equation:

$$f(x, \sigma, c) = e^{-\frac{(x-c)^2}{2\sigma^2}} \tag{11}$$

In this study, the position and width σ and $2c$ are selected as the optimization variables to further improve the performance of FVPC. Fig. 4 shows the MFs of the fuzzy variables SoC, G and P. The input variable SoC is represented by the following five MFs: very low (VL), low (L), medium (M), high (H), and very high (VH). M_1^s to M_5^s are used to describe the width of MFs and M_6^s to M_8^s are used to describe the positions. Similar to SoC, five MFs are adopted in G to describe the peak-shaving requirement of the grid: negative high (NH), negative medium (NM), medium (M), positive medium (PM), and positive high (PH). M_1^g to M_5^g are used to describe the width of MFs and M_6^g to M_8^g are used to describe the positions. Comparing with SoC and G, the output variable P is fuzzified into 7 fuzzy regions represented by linguistic variables to better refine the V2G power of GEVs: negative high (NH), negative medium (NM), negative low (NL), medium (M), positive low (PL), positive medium (PM) and positive high (PH). Meanwhile, 12 variables are used to move the width and positions of MFs. M_1^p to M_7^p are used to adjust the width while M_8^p to M_{12}^p are used to adjust the position of gauss member functions.

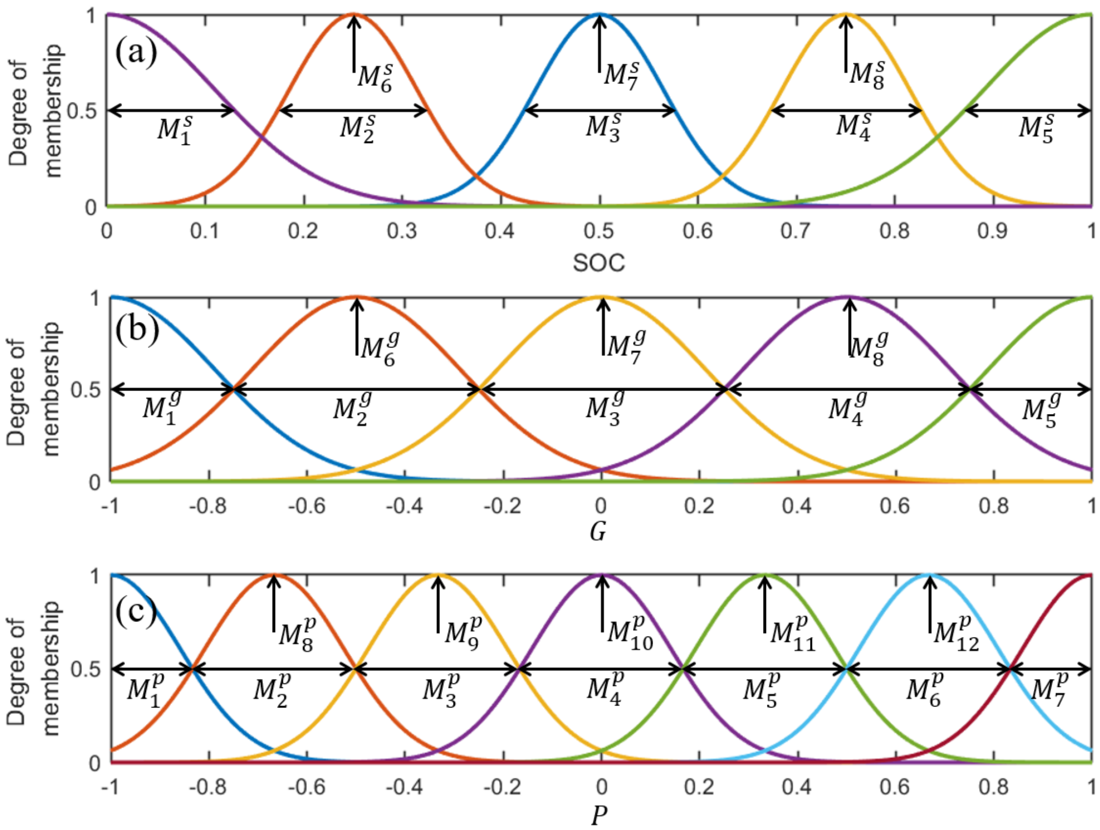

Fig. 4. Membership functions fuzzy variables. (a) Input variable SoC, (b) input variable G, (c) output variable P.

The output of the fuzzy controller is the V2G power of each GEVs, which is derived based on the fuzzy rules. Table I gives the rules used in the established FVPC. The energy storage capacity of GEVs is used to provide peak-shaving services to the grid based on the power balance state G and the battery state SoC. When grid peak power appears, the MFs of G: PM and PH are functioning, and the V2G power state is set as M to PH to schedule GEVs to discharge their energy storage capacity to the grid to provide peak-shaving service. On the contrary, when grid valley appears, the MFs of G: NM and NH will be functioning, and the V2G power state P is set as NH to M to absorb grid surplus power and improve energy efficiency by charging GEV batteries. The fuzzy battery state variable SoC is used to reflect the charging requirement of GEVs. When SoC is low (VL and L), the V2G power state P is set as NH to M to charge the battery and satisfy the charging requirement of participants. While when SOC is high (H and VH), the V2G power state is set as M to PH to provide peak-shaving services.

Table I. Rule base used in the established fuzzy V2G power coordinator.

G \ ***SOC*** ***P***	**VL**	**L**	**M**	**H**	**VH**
NH	NH	NH	NM	NL	M
NM	NH	NL	NL	M	M
M	NM	NL	M	PL	PM
PM	M	M	PL	PM	PH
PH	M	PL	PM	PH	PH

B. Parameter calibration based on the global optimized strategies

To improve the performance of the established FVPC, an optimization model is established in this part to search for the optimal width and position of MFs. The value of $\mathbf{M}^g$, $\mathbf{M}^s$ and $\mathbf{M}^p$ are further adjusted by utilizing the results of the optimization-based V2G scheduling model mentioned in Section III, and the optimization variable $\mathbf{M}$ is designed as follows:

$$\mathbf{M} = \begin{bmatrix} \mathbf{M}^s \\ \mathbf{M}^g \\ \mathbf{M}^p \end{bmatrix}^{\mathrm{T}} = \begin{bmatrix} M_1^s & \cdots & M_8^s & M_1^g & \cdots & M_8^g & M_1^p & \cdots & M_{12}^p \end{bmatrix} \tag{12}$$

The optimization objectives are to adjust the state of FVPC to get the optimal performance, and the results in the optimization-based V2G scheduling model are used as the reference signal. Firstly, to guarantee the FVPC can provide similar peak-shaving performance comparing to the optimization-based model, the first objective function is designed to minimize the difference between the aggregated V2G power provided by the FVPC and optimization-based model:

$$J_1 = \sum_{t=0}^{n} \sum_{i=1}^{m} f_c(G_t, SoC_{i,t}) - P_{i,t}^o \tag{13}$$

Where: f_c is the transfer function of the established FVPC, which is used to calculate the V2G power of GEVs based on the grid power balance state and GEV battery state. Furthermore, to mitigate the battery aging when participating in providing V2G services, the charging behaviors of a single V2G participant are also optimized in FVPC. The minimization of the difference between the battery SoC profile in the FVPC method and optimization-based scheduling model is designed as the second objective function:

$$J_2 = \sum_{t=0}^{n} \sum_{i=1}^{m} S_c(P_{i,t}) - S_c(P_{i,t}^o) \tag{14}$$

Where: S_c is the transfer function to calculate the battery SoC value based on the V2G power profile, as defined in equation (4). The fuzzy controller parameters calibration model is subjected to the following numerical constraints:

$$M_6^s \le M_7^s \le M_8^s \tag{15}$$

$$M_6^g \le M_7^g \le M_8^g \tag{16}$$

$$M_8^p \le M_9^p \le M_{10}^p \le M_{11}^p \le M_{12}^p \tag{17}$$

Equations (15) to (17) constrain the position of MFs to guarantee effectiveness by avoiding the peaks overlapping phenomenon between different gauss member functions.

V. Simulation environment and results analysis

In this section, the simulation environment and the data sources are firstly provided. Then the parameter calibration results will be illustrated and the performance of V2G scheduling will be qualitatively analyzed. At last, the peak-shaving and battery anti-aging performance of the developed V2G scheduling model will be quantitatively analyzed and compared with other methods.

A. Data set and simulation method description

The schematic of the studied power grid with real data source and GEVs penetration is shown in Fig. 5. The grid demand data used in this paper comes from the Stentaway Primary substation near Plymouth, on the south coast of the UK [43]. The approximate (latitude, longitude) coordinates are (50.364, -4.086). The data consists of commercial and residential power consumption profiles in Megawatts (MW) in a period of January 2018 to May 2018. The national household travel survey data [44] and the Monte Carlo model [45] are employed to simulate the travel demand and charging behavior of GEVs, including the grid-connected time, departure time, and charging requirements. The V2G behavior of 30 GEVs each with a 30kW·h battery is considered in this study to provide peak-shaving service to the grid.

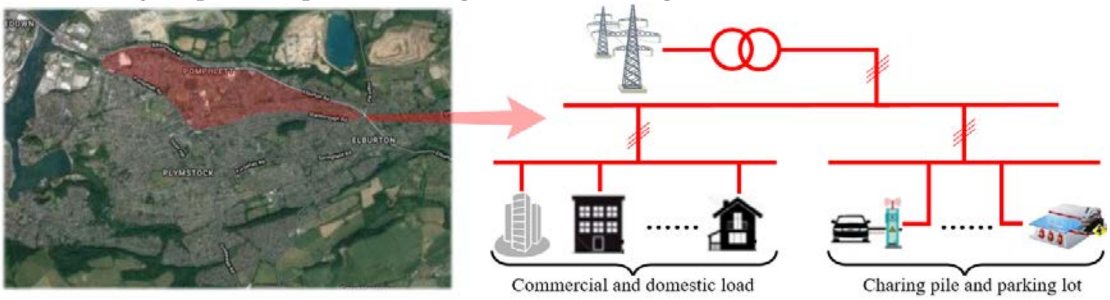

Fig. 5. The schematic of the studied power grid with real data sources.

Based on the above data, the charging behavior of GEVs is firstly scheduled by the established optimization-based V2G scheduling method. Then the derived V2G strategies, including the aggregated V2G power profile and vehicle battery SoC profile, are used to calibrate the parameters in the built FVPC. The historical grid load profiles within 120 days (from 1st January to 1st May in 2018) are used to calibrate the hyperparameter in the FVPC by the V2G strategies derived in the optimization-based scheduling model, as shown in Fig 6 (a). The performance of the established FVPC is verified by using grid load profiles in the same residential area but under a different period (from 2nd May to 1st June in 2018), as shown in (b). Grid demand peaks and valleys generally appear in the period of 16:00 to 21:00 and 21:00 to 08:00, respectively. Therefore, this paper mainly focuses on the period of 16:00 to 08:00 to deploy V2G services.

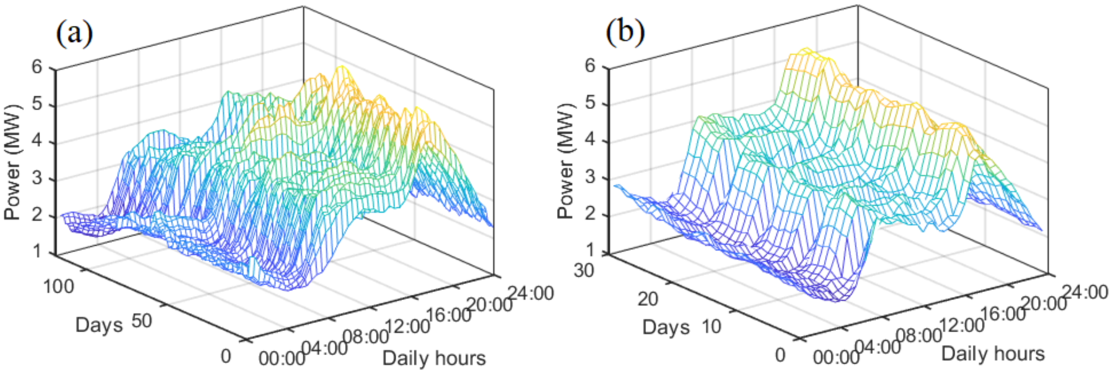

Fig. 6. Grid load profiles used in this paper to verify the performance of FVPC. (a) 120 historical profiles for parameter calibrating; (b) 30 profiles for model verification.

B. FVPC parameter calibration results

The adjusted width and position of MFs in FVPC before and after the parameter calibration process are compared in Fig. 7. Subfigure (a) shows the fuzzy regions adopted in the linguistic variable SoC, which is used to distinguish the battery energy state of GEVs. Compared to original MFs, the most remarkable change after the calibration is that the width of MFs in low and medium SOC states is greatly expanded. The value of M_1^s, M_2^s, and M_3^s are extended from 0.13, 0.16, and 0.16 to 0.18, 0.33, and 0.24 respectively. The extended width of these MFs improves the sensitivity of the established FVC to identify the low SOC state of the vehicle battery and thus can charge the battery timely to satisfy the charging requirement of participants. Meanwhile, the position of MFs is generally moved right to improve the degree of membership of low battery energy state and improve the charging speed. Similar to SoC, the fuzzy regions in linguistic variables G are also moved to improve the V2G scheduling performance. Compared to original MFs, the position of 'NM' is moved left from -0.45 to -0.64 while that of 'PM' is moved right from 0.45 to 0.62 to improve the recognition sensitivity of FVPC to grid peak-shaving and valley-filling requirements. With the calibrated rules, the established FVC can better follow the aggregated V2G power profile in the optimization-based model. When grid load levels are distinguished as 'PH',' PM',' NH', and' NM', the GEVs are scheduled to provide peak-shaving and valley-filling service, which will cause additional battery cycles. With the enlarged gaps between 'M' to 'NM' and 'M' to 'PM', the established FVC can clearly differ different grid peak-shaving requirement levels and provide more stable V2G strategies to avoid frequent change in battery charging and discharging states. Therefore, the additional battery cycles can be avoided and battery aging can be mitigated.

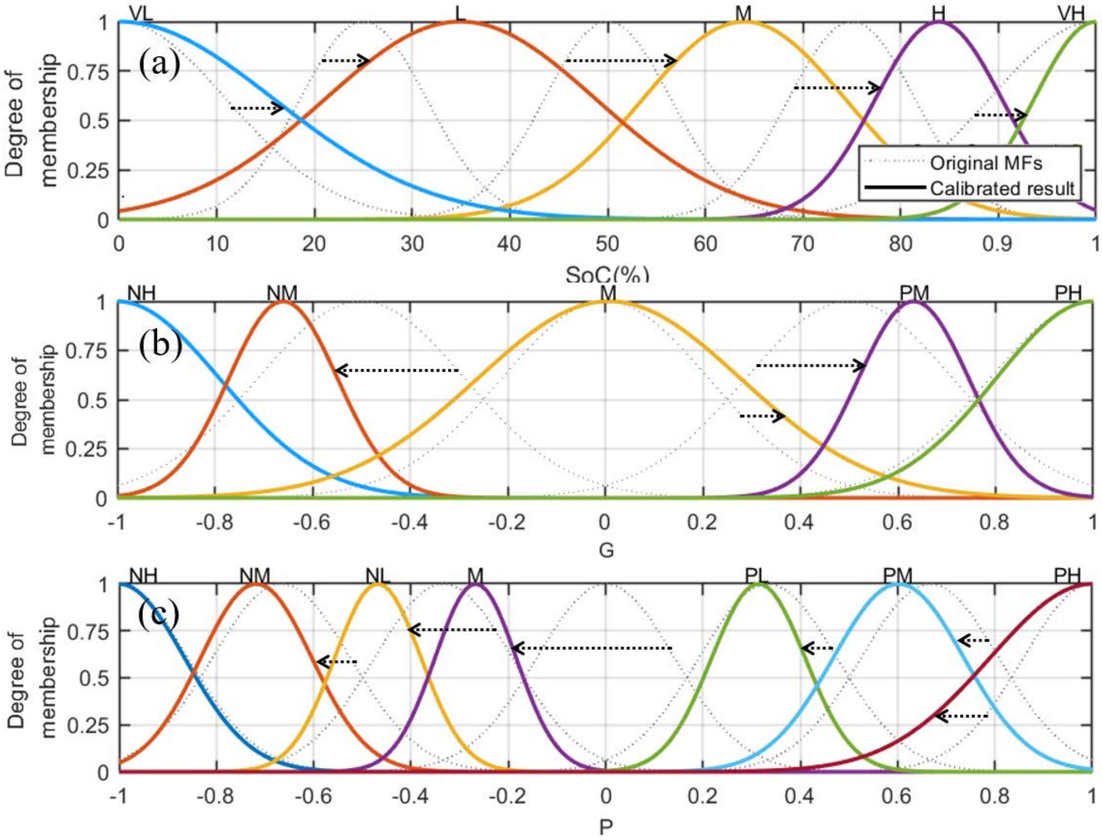

Fig. 7. The adjusted MFs in online V2G power controller after the parameter calibration process. (a) Input variable G, (b) input variable SoC, and (c) output variable P.

The fuzzy regions in the output variable: V2G power state P is also calibrated by the optimization-based V2G scheduling results. As shown in Fig. 7. (c), the most remarkable change is that the position of 'M',' NL', and' NM' are generally moved left. The FVPC is optimized by following the battery SoC profile in the optimization-based V2G scheduling results, and the left movement of MFs can schedule GEVs to be better and timely charged. Meanwhile, it is worth noting that the position of 'M', M_{12}^{p}, is optimized to the negative value (-0.24) from 0. The fuzzy region '0' frequently changes the battery charging state and thus can cause additional battery cycles. Therefore, M_{12}^{p} is optimized to a negative value to mitigate battery aging.

C. Analysis of peak-shaving and battery anti-aging performance

Fig. 8 shows the peak-shaving performance of the developed OPCF in a regular day under model verification dataset. Subfigure (b) compares the scheduled peak-shaving power in the optimization-based model and the calibrated rule-based model. Both two methods can respond to grid peak-shaving and valley-filling requirements. When grid load peaks at around 20:00 to 22:00, the GEVs are scheduled to provide peak-shaving service to the grid, the maximum V2G power reaches 460kW. While GEVs are scheduled to charge when grid valley appears after 24:00 to meet the charging requirement of V2G participants. The maximum aggregated charging power reaches -510kW from 02:00 to 05:00, which indicates that grid excess grid power generation capacity can be better utilized. After 06:00, the charging power is gradually reduced because most batteries have been fully charged and some GEVs have already been off-grid. The difference between the scheduled V2G power in the established FVPC and the optimization-based method can be limited to 42kw (4.2%), which validates the effectiveness of the developed parameter calibration method. Grid load profiles with and without GEVs penetration are compared in (a). With the developed OPCM method, the energy storage capacity in GEVs can be effectively utilized to reduce grid peak-valley difference. The grid peak-valley difference can be reduced from 1.72MW to 1.36MW, and load variance can be reduced from 0.3748 to 0.1605, which indicates the energy utilization efficiency can be significantly improved.

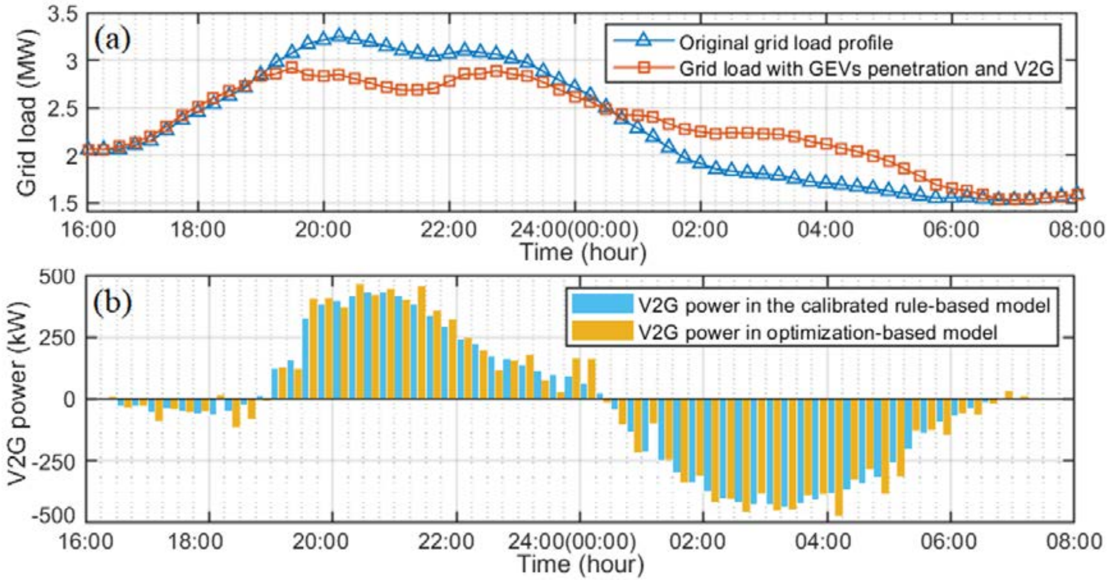

Fig. 8. The peak-shaving performance of the developed OPCF. (a) grid load profiles, (b) V2G power profiles.

The battery anti-aging performance of three different V2G scheduling methods: conventional fuzzy logic method [46], optimization-based method, and the calibrated fuzzy logic method under the verification dataset are compared in Table II. The battery percentage life loss calculation method in [47] is used here to evaluate the anti-aging performance. The V2G can be realized in the fuzzy logic method: more than 459.8kWh auxiliary power is provided to shave grid peak load profile on average. However, because lacking effective life protection mechanisms, the GEV batteries undertake 85 half-cycles and 176 full-cycles in the fleet. In a quantitative analysis for the single participant, more than 6.16×10^{-2}% of battery life is depleted. Compared to the fuzzy logic method, the optimal scheduling results can be derived in the optimization-based method. 27.8% more auxiliary power can be provided to reduce the grid peak-valley difference. Meanwhile, battery number of half-cycles and full-cycles in the GEVs fleet can be reduced to 63 and 92. From the perspective of a single participant, battery DOD decreases from 125% to 96% and more than 47.2% battery life loss can be avoided compared with conventional fuzzy logic method.

Table II. The battery anti-aging performance of different V2G scheduling methods.

Scenario	Fuzzy logic method	Optimization model	OPCF method
Average E_{disc}	459.8	582.9	570.4
Average E_{ch}	963.4	1262	1125.5
Average battery NHC	85	63	67
Average battery NFC	176	92	124
Average sum of DOD of a vehicle (%)	125	107	113
Average life loss of a vehicle ($\times 10^{-2}$%)	6.16	3.25	3.83

To enable the real-time applicability of the derived V2G strategies, the results in the optimization-based model are further used to calibrate rules in FVPC. After the parameter calibration process, the performance of the fuzzy logic method is significantly improved. As shown in Table II, the calibrated FVPC can achieve a similar performance compared with the optimization-based method. Compared to the conventional fuzzy logic method, an average of 24.1% more auxiliary power can be provided, while the battery number of half-cycles and full-cycles can be reduced to 124 and 107. As a result, the quantified average battery life loss of a single participant can be reduced by 37.8%, which validates that the battery aging mitigation performance of the developed OPCF method.

VI. Conclusion

An online battery anti-aging V2G scheduling method is developed in this paper for providing peak-shaving service to the grid. Based on the grid daily operation state information, including load profiles and GEVs charging requirements, the optimal charging strategies are derived by an optimization-based V2G scheduling model. Furthermore, an online FVPC and a rule extraction method are proposed to enable the online deployment of the derived optimal V2G strategies. Through extensive simulations, the key findings are as follows:

- The battery anti-aging can be better realized in an optimization-based V2G behavior management model. Compared to the rule-based method, more than 47.2% battery life loss can be avoided while providing the same peak-shaving service.
- The parameter calibration process can significantly improve the performance of the established rule-based V2G coordinator. With the developed parameter calibration method, the established online V2G coordinator can achieve a similar peak-shaving and battery anti-aging performance compared to the optimization-based model.
- Numerical analyses indicate that 24.1% more auxiliary power can be provided while the battery life loss can be reduced by 37.8% compared to the conventional fuzzy logic method.

In the developed OPCF method, historical grid demand profiles are required to optimize the hyper-parameters in the online fuzzy V2G power coordinator. In practical applications, the optimization process and the fuzzy logic V2G controller need to be carried out and trained for every single place. Future work can be conducted on improving the generalization ability of FVPC to adapt to the scenarios in different residential areas without parameter calibration processes.

References

[1] S. Cao, "The impact of electric vehicles and mobile boundary expansions on the realization of zero-emission office buildings," *Applied Energy,* vol. 251, p. 113347, 2019/10/01/ 2019.

[2] L. Jian, X. Zhu, Z. Shao, S. Niu, and C. C. Chan, "A scenario of vehicle-to-grid implementation and its double-layer optimal charging strategy for minimizing load variance within regional smart grids," *Energy Conversion and Management,* vol. 78, pp. 508-517, 2014/02/01/ 2014.

[3] M. Zhang, W. Li, S. S. Yu, K. Wen, C. Zhou, and P. Shi, "A unified configurational optimization framework for battery swapping and charging stations considering electric vehicle uncertainty," *Energy,* vol. 218, p. 119536, 2021/03/01/ 2021.

[4] Y. Luo, T. Zhu, S. Wan, S. Zhang, and K. Li, "Optimal charging scheduling for large-scale EV (electric vehicle) deployment based on the interaction of the smart-grid and intelligent-transport systems," *Energy,* vol. 97, pp. 359-368, 2016/02/15/ 2016.

[5] W. Kempton and J. J. J. o. p. s. Tomić, "Vehicle-to-grid power fundamentals: Calculating capacity and net revenue," vol. 144, no. 1, pp. 268-279, 2005.

[6] L. Jin, C.-K. Zhang, Y. He, L. Jiang, and M. Wu, "Delay-Dependent Stability Analysis of Multi-Area Load Frequency Control with Enhanced Accuracy and Computation Efficiency," *IEEE Transactions on Power Systems,* 2019.

[7] A. Kavousi-Fard, A. Abunasri, A. Zare, and R. Hoseinzadeh, "Impact of plug-in hybrid electric vehicles charging demand on the optimal energy management of renewable micro-grids," *Energy,* vol. 78, pp. 904-915, 2014/12/15/ 2014.

[8] C. D. White and K. M. Zhang, "Using vehicle-to-grid technology for frequency regulation and peak-load reduction," *Journal of Power Sources,* vol. 196, no. 8, pp. 3972-3980, 2011/04/15/ 2011.

[9] P. Li, W. Hu, X. Xu, Q. Huang, Z. Liu, and Z. Chen, "A frequency control strategy of electric vehicles in microgrid using virtual synchronous generator control," *Energy,* vol. 189, p. 116389, 2019/12/15/ 2019.

[10] K. M. Tan, S. Padmanaban, J. Y. Yong, and V. K. Ramachandaramurthy, "A multi-control vehicle-to-grid charger with bi-directional active and reactive power capabilities for power grid support," *Energy,* vol. 171, pp. 1150-1163, 2019/03/15/ 2019.

[11] Y. Wang, Z. Yang, M. Mourshed, Y. Guo, Q. Niu, and X. Zhu, "Demand side management of plug-in electric vehicles and coordinated unit commitment: A novel parallel competitive swarm optimization method," *Energy Conversion and Management,* vol. 196, pp. 935-949, 2019/09/15/ 2019.

[12] Y. Shang, M. Liu, Z. Shao, and L. Jian, "Internet of smart charging points with photovoltaic Integration: A high-efficiency scheme enabling optimal dispatching between electric vehicles and power grids," *Applied Energy,* vol. 278, p. 115640, 2020/11/15/ 2020.

[13] H. Kamankesh, V. G. Agelidis, and A. Kavousi-Fard, "Optimal scheduling of renewable micro-grids considering plug-in hybrid electric vehicle charging demand," *Energy,* vol. 100, pp. 285-297, 2016/04/01/ 2016.

[14] T. Xu *et al.*, "Considering the Life-Cycle Cost of Distributed Energy-Storage Planning in Distribution Grids," vol. 8, no. 12, p. 2615, 2018.

[15] L. Luo, Z. Wu, W. Gu, H. Huang, S. Gao, and J. Han, "Coordinated allocation of distributed generation resources and electric vehicle charging stations in distribution systems with vehicle-to-grid interaction," *Energy,* vol. 192, p. 116631, 2020/02/01/ 2020.

[16] K. M. Tan, V. K. Ramachandaramurthy, and J. Y. Yong, "Optimal vehicle to grid planning and scheduling using double layer multi-objective algorithm," *Energy,* vol. 112, pp. 1060-1073, 2016/10/01/ 2016.

[17] S. Khemakhem, M. Rekik, and L. Krichen, "A flexible control strategy of plug-in electric vehicles operating in seven modes for smoothing load power curves in smart grid," *Energy,* vol. 118, pp. 197-208, 2017/01/01/ 2017.

[18] C. Zhou, K. Qian, M. Allan, and W. J. I. T. o. E. C. Zhou, "Modeling of the cost of EV battery wear due to V2G application in power systems," vol. 26, no. 4, pp. 1041-1050, 2011.

[19] Y. Zhou, S. Cao, J. L. M. Hensen, and A. Hasan, "Heuristic battery-protective strategy for energy management of an interactive renewables–buildings–vehicles energy sharing network with high energy flexibility," *Energy Conversion and Management,* vol. 214, p. 112891, 2020/06/15/ 2020.

[20] M. Ebrahimi, M. Rastegar, M. Mohammadi, A. Palomino, and M. J. I. T. o. T. E. Parvania, "Stochastic Charging Optimization of V2G-Capable PEVs: A Comprehensive Model for Battery Aging and Customer Service Quality," vol. 6, no. 3, pp. 1026-1034, 2020.

[21] Y. He, B. Venkatesh, and L. Guan, "Optimal Scheduling for Charging and Discharging of Electric Vehicles," *IEEE Transactions on Smart Grid,* vol. 3, no. 3, pp. 1095-1105, 2012.

[22] A. R. Bhatti and Z. J. R. e. Salam, "A rule-based energy management scheme for uninterrupted electric vehicles charging at constant price using photovoltaic-grid system," vol. 125, pp. 384-400, 2018.

[23] A. Ahmadian, M. Sedghi, A. Elkamel, M. Fowler, M. A. J. R. Golkar, and S. E. Reviews, "Plug-in electric vehicle batteries degradation modeling for smart grid studies: Review, assessment and conceptual framework," vol. 81, pp. 2609-2624, 2018.

[24] H. Krueger and A. Cruden, "Multi-Layer Event-Based Vehicle-to-Grid (V2G) Scheduling With Short Term Predictive Capability Within a Modular Aggregator Control Structure," *IEEE Transactions on Vehicular Technology,* vol. 69, no. 5, pp. 4727-4739, 2020.

[25] M. Ihara, S. Tianmeng, and H. Nishi, "A simulation study of electric power leveling using V2G infrastructure," in *IECON 2011 - 37th Annual Conference of the IEEE Industrial Electronics Society*, 2011, pp. 3224-3229.

[26] H. C. Hesse, M. Schimpe, D. Kucevic, and A. J. E. Jossen, "Lithium-ion battery storage for the grid—A review of stationary battery storage system design tailored for applications in modern power grids," vol. 10, no. 12, p. 2107, 2017.

[27] Z. Huang, B. Fang, J. J. P. Deng, and C. o. M. P. Systems, "Multi-objective optimization strategy for distribution network considering V2G-enabled electric vehicles in building integrated energy system," vol. 5, no. 1, p. 7, 2020.

[28] G. Buja, M. Bertoluzzo, and C. J. I. t. o. p. e. Fontana, "Reactive power compensation capabilities of V2G-enabled electric vehicles," vol. 32, no. 12, pp. 9447-9459, 2017.

[29] S. Aghajani and M. Kalantar, "A cooperative game theoretic analysis of electric vehicles parking lot in smart grid," *Energy,* vol. 137, pp. 129-139, 2017/10/15/ 2017.

[30] S. Li, C. Gu, J. Li, H. Wang, and Q. Yang, "Boosting Grid Efficiency and Resiliency by Releasing V2G Potentiality Through a Novel Rolling Prediction-Decision Framework and Deep-LSTM Algorithm," *IEEE Systems Journal,* vol. 15, no. 2, pp. 2562-2570, 2021.

[31] M. Ebrahimi, M. Rastegar, M. Mohammadi, A. Palomino, and M. Parvania, "Stochastic Charging Optimization of V2G-Capable PEVs: A Comprehensive Model for Battery Aging and Customer Service Quality," *IEEE Transactions on Transportation Electrification,* vol. 6, no. 3, pp. 1026-1034, 2020.

[32] H. Farzin, M. Fotuhi-Firuzabad, and M. Moeini-Aghtaie, "A Practical Scheme to Involve Degradation Cost of Lithium-Ion Batteries in Vehicle-to-Grid Applications," *IEEE Transactions on Sustainable Energy,* vol. 7, no. 4, pp. 1730-1738, 2016.

[33] K. Thirugnanam, E. R. J. TP, M. Singh, and P. J. I. t. o. E. c. Kumar, "Mathematical modeling of Li-ion battery using genetic algorithm approach for V2G applications," vol. 29, no. 2, pp. 332-343, 2014.

[34] A. Zakariazadeh, S. Jadid, and P. Siano, "Multi-objective scheduling of electric vehicles in smart distribution system," *Energy Conversion and Management,* vol. 79, pp. 43-53, 2014/03/01/ 2014.

[35] J. Wang, J. Wang, Q. Wang, and X. J. J. o. t. F. I. Zeng, "Control rules extraction and parameters optimization of energy management for bus series-parallel AMT hybrid powertrain," vol. 355, no. 5, pp. 2283-2312, 2018.

[36] P. May-Ostendorp, G. P. Henze, C. D. Corbin, B. Rajagopalan, C. J. B. Felsmann, and Environment, "Model-predictive control of mixed-mode buildings with rule extraction," vol. 46, no. 2, pp. 428-437, 2011.

[37] J. Peng, H. He, and R. Xiong, "Rule based energy management strategy for a series–parallel plug-in hybrid electric bus optimized by dynamic programming," *Applied Energy,* vol. 185, pp. 1633-1643, 2017/01/01/ 2017.

[38] N. Erdogan, F. Erden, M. J. J. o. M. P. S. Kisacikoglu, and C. Energy, "A fast and efficient coordinated vehicle-to-grid discharging control scheme for peak shaving in power distribution system," vol. 6, no. 3, pp. 555-566, 2018.

[39] C. Chen, Z. Yang, J. He, H. Tian, S. Li, and D. J. J. o. V. Wang, "Load spectrum generation of machining center based on rainflow counting method," vol. 19, no. 8, pp. 5767-5779, 2017.

[40] S. Li, C. Gu, P. Zhao, and S. Cheng, "Adaptive energy management for hybrid power system considering fuel economy and battery longevity," *Energy Conversion and Management,* vol. 235, p. 114004, 2021/05/01/ 2021.

[41] Q. Badey, G. Cherouvrier, Y. Reynier, J. Duffault, and S. J. C. T. E. Franger, "Ageing forecast of lithium-ion batteries for electric and hybrid vehicles," vol. 16, pp. 65-79, 2011.

[42] J. Wang, W. Zhang, and J. Zhang, "Cooperative Differential Evolution With Multiple Populations for Multiobjective Optimization," *IEEE Transactions on Cybernetics,* vol. 46, no. 12, pp. 2848-2861, 2016.

[43] " https://www.westernpower.co.uk/innovation/pod/dataset/data-licences," ed.

[44] U. D. o. Transportation, "National household travel survey," ed: Federal Highway Administration Washington, DC, 2009.

[45] R. J. Bessa and M. J. E. P. S. R. Matos, "Global against divided optimization for the participation of an EV aggregator in the day-ahead electricity market. Part II: Numerical analysis," vol. 95, pp. 319-329, 2013.

[46] M. Singh, P. Kumar, and I. Kar, "Implementation of Vehicle to Grid Infrastructure Using Fuzzy Logic Controller," *IEEE Transactions on Smart Grid,* vol. 3, no. 1, pp. 565-577, 2012.

[47] B. Xu, J. Zhao, T. Zheng, E. Litvinov, and D. S. Kirschen, "Factoring the Cycle Aging Cost of Batteries Participating in Electricity Markets," *IEEE Transactions on Power Systems,* vol. 33, no. 2, pp. 2248-2259, 2018.